

THERMAL INERTIA USING THEMIS INFRARED DATA. R. L. Fergason and P. R. Christensen, Department of Geological Sciences, Mars Space Flight Facility, Arizona State University, Box 876305, Tempe, AZ 85287-6305, robin.fergason@asu.edu.

Introduction: Many landforms observed in Mars Orbiter Camera (MOC) narrow-angle images are too small to detect using Mars Global Surveyor Thermal Emission Spectrometer (TES) thermal inertia data. This makes the task of studying the thermophysical properties of features undetectable at TES resolution (3 km per pixel), such as inter-crater deposits, inter-channel deposits, and small-scale surface characteristics, unfeasible. Therefore, the understanding of physical processes that have recently affected the martian surface is limited. In this study, a method was developed to produce high-resolution (100 meters per pixel) thermal inertia maps by calculating thermal inertia values using Mars Odyssey Thermal Emission Imaging System (THEMIS) night-IR temperature data. These maps provide high-resolution thermophysical information, which is necessary to further understand smaller surface features and the recent aeolian processes that produced these landforms.

Thermal inertia is a physical property of the upper tens of centimeters of the surface material that controls both the diurnal variations in surface temperature, and the ability of the subsurface to store or conduct heat. It is a model-derived parameter based on the surface's response to changes in temperature throughout the day [1, 2, 3, 4, 5]. Thermal inertia is defined as $I=(\rho kc)^{1/2}$, where ρ is the bulk density, k is the thermal conductivity, and c is the specific heat of the surface material. The thermal conductivity of a material has the greatest influence on thermal inertia, and the average particle size is determined from this relationship [6, 7, 8]. To first order, regions with a low thermal inertia consist of fine-grained (less than 150 μm) surface material and as the thermal inertia increases, so does the surface particle size. However, this relationship can be complicated due to factors such as the mixing of particle sizes and the presence of suspected duricrusts [9].

Approach: A method was developed to calculate the thermal inertia at THEMIS night-IR resolution. The radiance from THEMIS night-IR images was converted to surface brightness temperatures. Then, for each individual image, a look-up table of temperatures and their corresponding thermal inertia values was created for a given latitude, L_s , albedo, local time of day, and elevation. The table values were calculated using a thermal model [10] similar to those developed for Viking IRTM [1] and MGS-TES [2]. THEMIS nighttime temperature images were converted to thermal inertia using the created look-up table. The parameters this method assumes are constant within a single image include: latitude, L_s , local time of day, elevation, and albedo. Because of these assumptions, this technique should be used with caution when dramatic elevation changes (several 100 meters) occur within an image. Also, since albedo has negligible effects on surface temperature at night, it does not dramatically effect the thermal inertia calculations. This method is applied to THEMIS nighttime temperature images to analyze thermophysical features that are undetectable at TES resolution. This technique provides higher resolution

information that allows improved quantitative studies of small-scale surface features and a better understanding of the geological processes that have produced these surface characteristics.

Results: THEMIS thermal inertia images provide higher-resolution information, and we are now able to distinguish small-scale features (smaller than TES detection limits) observed in MOC images using this technique. This example is from the Tharsis region northeast of the volcano complex and west of Kasei Vallis (center longitude ~ 287 E, center latitude ~ 22.5 N). THEMIS thermal inertia values provide realistic data results, and, in this region, correspond well with TES thermal inertia data ranges. Figure 1a is a mosaic of THEMIS thermal-inertia images created using the method discussed above. The surface particle size range in this mosaic is dust (blue) to medium sand (red). Dust (thermal inertia between 40 and 150) is the most abundant material in this region, as expected from TES results, and blankets much of the surface. Elevated thermal inertia values (250 to 425), which correspond to sand-sized particles, occur on crater rims and on the rims and sides of channels. This implies that the slopes of these surfaces may be too steep for dust to accumulate. Often, channel sides have elevated thermal inertia values. However, depressions displaying a lower thermal signature on the walls and floors, suggesting the presence of dust, are also observed. Figure 2 is an example of this phenomenon. In this MOC image, dunes exist in some depressions (Figure 1b provides the regional context of the channel locations). These dunes do not correspond to elevated thermal inertia values (which would indicate a larger particle size, as expected), but instead occur in depressions containing low thermal inertia values. Two possible explanations are that either these dunes are covered in a layer of dust and are not currently active, or they consist of a porous material.

Conclusion and Future Work: THEMIS provides realistic thermal inertia values. In the northeastern Tharsis region, similar thermal inertia values were observed with TES, but THEMIS allows for a higher resolution, quantitative analysis of both surface features and the particle sizes present. Currently, additional sites are being analyzed to corroborate the results of this model, and to compare THEMIS thermal inertia results with values detected using TES. We are also using this technique to study variable aeolian features in low thermal inertia regions, primarily in Arabia Terra.

References: [1] Kieffer H. H. et al. (1977) *JGR*, 82, 4249-4291. [2] Mellon M. T. et al. (2000) *Icarus*, 148, 437-455. [3] Palluconi F. D. and Kieffer H. H. (1981) *Icarus*, 45, 415-426. [4] Jakosky B. M. et al. (2000) *JGR*, 105, 9643-9652. [5] Christensen P. R. and Moore H. J. (1992) in *Mars*, edited by H. H. Kieffer et al., Univ. of AZ Press, 686-729. [6] Wechsler A. E. and Glaser P. E. (1965) *Icarus*, 4, 335-352. [7] Presley M. A. and Christensen P. R. (1997) *JGR*, 102, 6551-6566. [8] Jakosky B. M. and Christensen P. R. (1986) *JGR*, 91, 3547-3559. [9] Jakosky B. M. (1986)

Icarus, 66, 117-124. [10] H. H. Kieffer, personal communication, 2003.

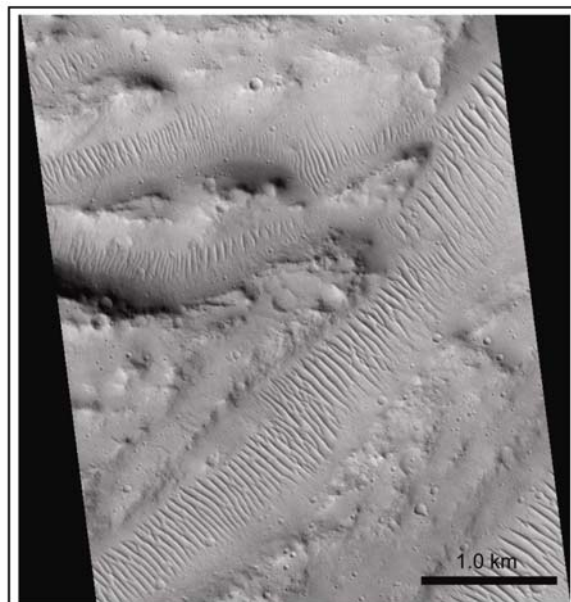
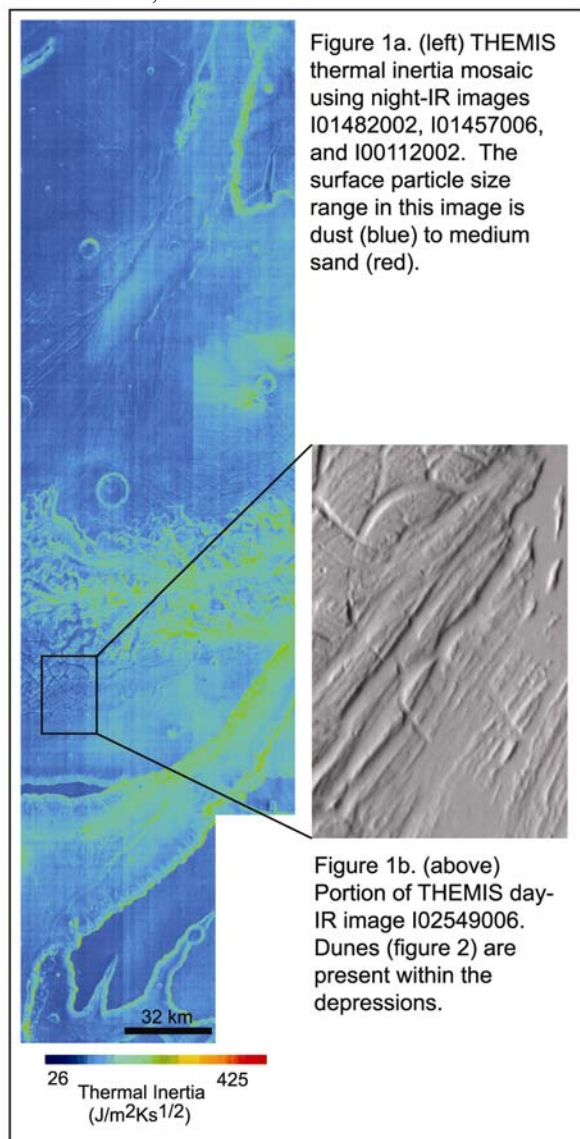


Figure 2. Dunes present in MOC narrow-angle image M0802252 are located in depressions consisting of low-thermal inertia material.